Eur. J. Mineral.
2008, **20**, 271–280
Published online February 2008

Skorpionite, $Ca_3Zn_2(PO_4)_2CO_3(OH)_2 \cdot H_2O$, a new mineral from Namibia: description and crystal structure

WERNER KRAUSE[1,*], HERTA EFFENBERGER[2], HEINZ-JÜRGEN BERNHARDT[3] and OLAF MEDENBACH[3]

[1] Henriette-Lott-Weg 8, 50354 Hürth, Germany
*Corresponding author, e-mail: We.Krause@t-online.de
[2] Institut für Mineralogie und Kristallographie, Universität Wien, Geozentrum, Althanstraße 14, 1090 Wien, Austria
[3] Institut für Mineralogie, Ruhr-Universität Bochum, Universitätsstraße 150, 44780 Bochum, Germany

Abstract: Skorpionite, $Ca_3Zn_2(PO_4)_2CO_3(OH)_2 \cdot H_2O$, is a new secondary mineral from the Skorpion zinc deposit in south-western Namibia. Associated minerals are tarbuttite, hydrozincite and gypsum. Skorpionite forms colourless needle-like crystals of monoclinic symmetry that are elongated parallel to [001] with dominant {100} and {110}; additional forms are {111}, {221}, {131} and {–101}. D (meas.) = 3.15(3) g/cm^3; D (calc.) = 3.17 g/cm^3. Skorpionite is optically biaxial negative, α = 1.5884(10), β = 1.6445 (calc.), γ = 1.6455(10), 2V = 15.0°(5) (589 nm); no dispersion. Optical orientation is Y ^ c = 26° (in acute β); $Z = b$. Means of 17 sets of microprobe analyses gave CaO 30.89, ZnO 28.83, P_2O_5 25.49, CO_2 (calc.) 7.96, H_2O (calc.) 6.52, total 99.69 wt.%. The empirical formula (based on 14 oxygen atoms *pfu*) is $Ca_{3.05}Zn_{1.96}(PO_4)_{1.99}(CO_3)_{1.00}(OH)_{2.06} \cdot 0.98H_2O$. Single-crystal X-ray investigations gave space group $C2/c$, with unit-cell parameters a = 19.045(3), b = 9.320(2), c = 6.525(1) Å, β = 92.73(2)°, V = 1156.9(4) Å^3, Z = 4. ZnO_4 and PO_4 tetrahedra are corner linked to corrugated sheets. The crystal structure forms a three-dimensional network of $[Ca2_2Zn_2(OH)_2(PO_4)_2]^0$ and $[Ca1(CO_3)(H_2O)]^0$ layers that are linked by hydrogen bonds and by Ca–O bonds.

Key-words: skorpionite, new mineral, Skorpion mine, Namibia, microprobe analysis, crystal structure, calcium zinc carbonate-phosphate hydroxyhydrate.

Introduction

In the course of an investigation of specimens from the Skorpion zinc mine in Namibia a few samples with colourless needle-like crystals were found which could not be identified by means of an X-ray powder diffraction pattern. Microchemical tests showed calcium, zinc, phosphate and carbonate as major components and thus indicating the presence of a possibly new mineral. Subsequent single-crystal X-ray studies and microprobe analyses confirmed this material to be a new species. It has been named skorpionite after the type locality. Mineral and mineral name have been approved by the IMA commission on New Minerals and Mineral Names (IMA 2005-010). Type material is preserved in the collection of the Mineralogical Institute, University of Bochum, Germany, under catalogue number IMA 2005-010.

Occurrence

The Skorpion zinc mine (27°49' S, 16°36' E, elevation 660 m) is a non-sulphide ore deposit that is located in south-western Namibia, approximately 40 km northwest of the Orange river and some 20 km northwest of the Rosh Pinah mine, Lüderitz district, Karas region, Namibia, Africa. Access to the mine is limited, because it is situated within Namibia's Diamond Area 1, the so-called "Sperrgebiet" (Jacob *et al*., 2006). The Skorpion zinc deposit comprises a non-sulphide orebody (24.6 Mt at 10.6 wt.% Zn) which has been formed by the supergene oxidation of Neoproterozoic sediment- and volcanic-hosted disseminated sulphides in the Pan-African Gariep Belt (Borg *et al*., 2003). The host rocks have been strongly folded, faulted and overprinted by lower amphibolite facies metamorphism. The dominant ore minerals are hemimorphite, smithsonite, sauconite and hydrozincite. These minerals occur as open space fillings in intergranular voids, fractures and breccias and as replacements of feldspar and mica mainly in the arkosic metarenites and subordinately in the volcanoclastic metasedimentary rocks. Details of the geology, the mineralogy and the genesis of the Skorpion zinc deposit were compiled by Kärner (2006). A brief description of the ore minerals was given by Kärner *et al*. (2002).

Currently, zinc is produced mostly from zinc sulphide ores because sulphides are easy to separate from gangue and to concentrate by conventional flotation techniques. As new sphalerite mines are becoming more difficult to find,

DOI: 10.1127/0935-1221/2008/0020-1789
0935-1221/08/0020-1789 $ 4.50

new processes to produce zinc metal from oxidized zinc ores are being developed. Processing of such ore material is done by the SXEW process (Solvent Extraction Electrowinning) and involves 4 steps: (I) leaching the zinc bearing ore with sulphuric acid, (II) extraction of the zinc by an organic zinc complexing reagent, (III) extraction of the zinc from the organic extraction solution into the electrolyte solution, and (IV) electrolysis. The extraction reaction is reversible by controlling the p_H value (acidity). Prior to the development of the zinc solvent extraction process, oxide zinc minerals could not be economically processed. The SXEW process has been used for the production of copper for 30 years; it reduces the cost of producing zinc and copper by about 30 % compared to the smelter process. However, essentially all zinc and 80 % of copper production is still produced by the smelter process. The Skorpion mine is the first zinc production test of the SXEW process. Construction started in May 2001; the mine is in operation since 2003 (Sole *et al*., 2005).

Information about the mineral assemblage of the Skorpion mine has been given by Borg *et al*. (2003). The predominant supergene non-sulphide zinc mineral is sauconite; other frequently occurring zinc minerals are hemimorphite, smithsonite, hydrozincite, tarbuttite, scholzite, chalcophanite and hydrohetearolite. Secondary copper minerals are malachite, chrysocolla, atacamite and minor azurite.

The present study is based on rock samples that were collected by L. Krahn together with G. Borg and K. Kärner during a visit of the Skorpion mine in October 2003. The visit was part of a research programme and collaboration between the owner of the mine Anglo American plc and the Economic Geology and Petrology Research Group of the Martin-Luther University Halle-Wittenberg, Germany. The investigated samples can be attributed to the following three different subgroups:

Tarbuttite samples: The tarbuttite samples mainly consist of intergrown light-green tabular tarbuttite crystals up to 20 mm in size partly grown on colourless crusts of smithsonite; globular white aggregates of hydrozincite are grown on tarbuttite; minor parts of the specimens are covered with a thin colourless coating of gypsum; rarely, small colourless crystals of hemimorphite up to 3 mm and scholzite are grown on tarbuttite. Colourless needle-like crystals of the new mineral skorpionite could be identified on three of the tarbuttite samples.

Zinc carbonate samples: Zinc carbonate samples show white coatings consisting of very small thin-tabular crystals of hydrozincite that are grown on colourless crusts of smithsonite together with hemimorphite crystals. Rarely, small white scalenoedric crystals of calcite could be identified.

Copper mineral samples: Traces of a copper mineralization are widespread. Green crusts covered by a thin transparent coating of gypsum were identified as zincolibethenite, a new secondary mineral recently described by Braithwaite *et al*. (2005). In addition paratacamite could be identified as emerald-green tabular crystals grown on zincolibethenite nearly completely overgrown by gypsum. Zincolibethenite also occurs as light green-blue globular aggregates up to 1 cm overgrown with small well developed emerald-green crystals that turned out to be herbertsmithite, a new secondary copper-zinc-hydroxide-chloride, also recently described by Braithwaite *et al*. (2004). Empirical formulas based on microprobe data and unit-cell parameters refined from powder diffraction data for zincolibethenite and herbertsmithite from the Skorpion mine are given in the following. Herbertsmithite: $Cu_{3.38}Zn_{0.62}(OH)_{5.99}Cl_{2.01}$; trigonal rhombohedral; a = 6.8361(4), c = 14.070(1) Å, V = 569.4(1) Å^3. Zincolibethenite: $Cu_{0.95}Zn_{1.09}(PO_4)_{0.98}(OH)_{1.02}$; orthorhombic; a = 8.295(3), b = 8.314(6), c = 5.862(4) Å, V = 404.3(2) Å^3.

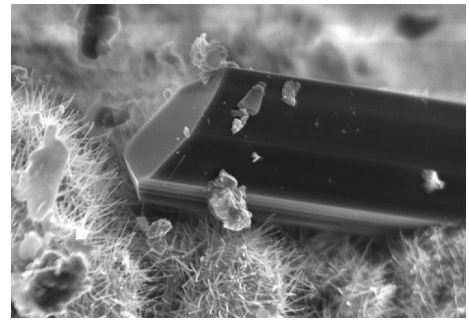

Fig. 1. Skorpionite crystal – SEM micrograph; picture width is 80 μm.

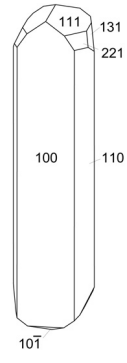

Fig. 2. Crystal drawing of skorpionite.

Physical properties

Skorpionite forms mostly individual needle-like crystals up to 0.5 mm in length and up to 40 μm in width; the mean aspect ratio is approximately 20:1. Morphology and optical orientation were determined by a combined measurement with an optical two-circle goniometer and a spindle stage. The crystals are elongated parallel to [001] with dominant {100} and {110}; additional forms are {111}, {221}, {131} and {$\bar{1}$01} (Fig. 1 and 2). No twinning was observed. Skorpionite is colourless with a white streak; it is transparent, the lustre is vitreous and there is no fluorescence in either long- or short-wave ultraviolet radiation. The Mohs' hardness is 3½. Skorpionite is brittle, fracture is uneven and no cleavage was observed. The density

Table 1. Electron microprobe analyses[1] of skorpionite (in wt.%).

	Mean[2]	Range	e.s.d.	calc.[3]
CaO	30.89	30.31–31.53	0.30	30.42
ZnO	28.83	27.72–30.11	0.62	29.43
P_2O_5	25.49	25.15–25.79	0.19	25.67
CO_2 [3]	7.96			7.96
H_2O [3]	6.52			6.52
Total	99.69			100.00

[1] Microprobe standards: ZnO (Zn), andradite (Ca), $AlPO_4$ (P).
[2] Means of 17 sets of electron-microprobe analyses; empirical formula: $Ca_{3.05}Zn_{1.96}(PO_4)_{1.99}(CO_3)_{1.00}(OH)_{2.06}\cdot 0.98H_2O$.
[3] Calculated for the ideal formula $Ca_3Zn_2(PO_4)_2CO_3(OH)_2\cdot H_2O$.

is 3.15(3) g/cm^3; it was measured by flotation in a mixture of methylene iodide and tetrabromoethane. The calculated density is 3.17 g/cm^3 (from empirical formula and single-crystal data). Skorpionite is optically biaxial negative, α = 1.5884(10), β = 1.6445(calc.), γ = 1.6455(10), 2V = 15.0°(5) (589 nm); no dispersion could be observed. The optical orientation is Y ^ c = 26° (in the acute angle β); $Z = b$.

Chemical analyses

Chemical analyses (Table 1) were carried out by means of an electron microprobe (WDS mode, 20 kV, 10 nA, 5 μm beam diameter). No other elements with atomic numbers greater than 8 could be detected. Due to lack of suitable material H_2O and CO_2 could not be determined directly. Both constituents were determined by infrared and Raman spectroscopy (qualitatively) and by crystal-structure determination. In addition, CO_2 was confirmed by microchemical tests. Skorpionite is easily dissolved in dilute hydrochloric acid with effervescence of carbon dioxide. The empirical formula (calculated from the microprobe results based on 14 oxygen atoms *pfu*) is $Ca_{3.05}Zn_{1.96}(PO_4)_{1.99}(CO_3)_{1.00}(OH)_{2.06}\cdot 0.98H_2O$. The simplified formula is $Ca_3Zn_2(PO_4)_2CO_3(OH)_2\cdot H_2O$, which requires: CaO 30.42, ZnO 29.43, P_2O_5 25.67, CO_2 7.96, H_2O 6.52, Total 100.00 wt.%. The compatibility according to the Gladstone-Dale relationship (Mandarino, 1981) is 0.009 (which is rated as superior).

The presence of hydroxyl groups, molecular water and of carbonate could be confirmed by Fourier-transform infrared (FTIR) and laser-Raman spectra. The IR spectrum (Fig. 3) was recorded with a Nicolet 5PC FTIR using a diamond microcell (resolution ± 2 cm^{-1}, random sample orientation). The spectrum shows a broad absorption band of weak intensity between 3450 and 3100 cm^{-1} due to the stretching vibration of hydroxyl groups and the water molecules. There is a medium absorption at 1638 cm^{-1} typical for the bending mode of molecular water. Strong absorption bands at 1459 and 1367 cm^{-1} are due to the carbonate group. Very strong absorptions at 1095, 1044, 1024 cm^{-1} and several medium to strong absorptions in the range of 900 to 400 cm^{-1} are mainly due to the phosphate group.

Raman spectra (Fig. 4) were collected by using a Renishaw RM1000 confocal edge filter-based micro-Raman system in the spectral range from 50 to 4000 cm^{-1}. The 488/514.5/632.8 nm excitation line of a ~ 20 mW Ar-ion/Ar-ion/HeNe laser was focused with a 50× /0.75 objective lens on the sample surface. The backscattered radiation (180° configuration) was analyzed with a 1200 lines/mm grating monochromator in the so-called "static grating scan" data collection mode. Raman intensities were collected for 300 s with a thermo-electrically cooled CCD array detector. The resolution of the system ("apparatus function") was 6/5/4 cm^{-1}, the wavenumber accuracy was ±1 cm^{-1} (both calibrated with the Rayleigh line and the 520.5 cm^{-1} line of a Si standard). Instrument control and data acquisition were done with Grams/32 software (Galactic Ind. Corp.). Because of the identical appearance of the spectra at different excitation wavelengths, the resulting band pattern can be unambiguously assigned to Raman-active vibrations (in contrast to inconvenient luminescence bands). There is a strong and broad Raman absorption due to hydroxyl groups between 3770 and 3100 cm^{-1} with a maximum at 3566 cm^{-1}. The absorption of molecular water is at 1633 cm^{-1}, in perfect agreement

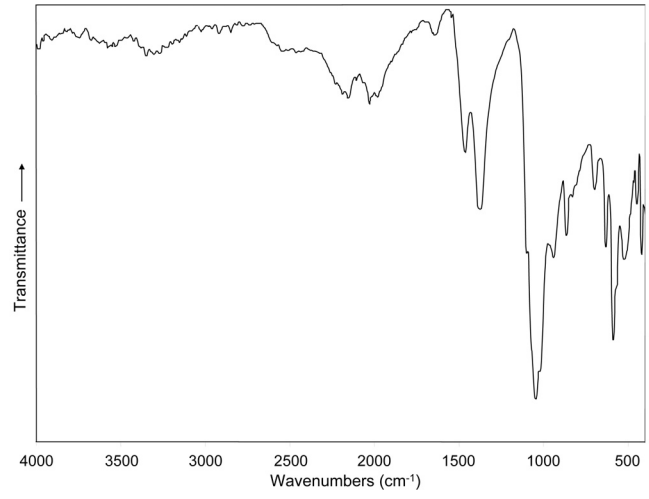

Fig. 3. Infrared spectrum of skorpionite. See text for band positions.

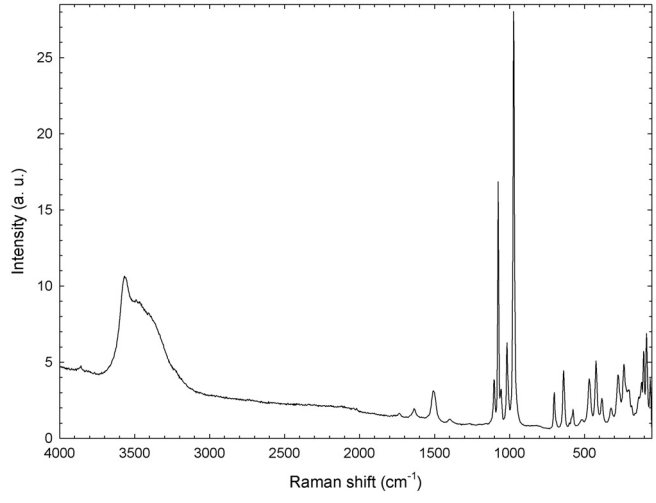

Fig. 4. Raman spectrum of skorpionite. See text for band positions.

with the IR data. Medium to weak absorptions at 1505 and 1398 cm^{-1} are due to the carbonate group. There are two very strong and sharp absorptions at 1075 and 972 cm^{-1} due to phosphate and additional medium absorptions at 1102, 1054, 1016, 702, 639, 575, 468, 423, 384, 322, 276 and 237 cm^{-1}.

X-ray investigation

X-ray powder diffraction data

X-ray powder diffractometer data are compiled in Table 2. There are a few additional reflections of relatively small intensity caused by minor impurities of tarbuttite. These additional reflections (d = 6.150; 2.778; 2.055 Å) have been omitted in Table 2. An unequivocal indexing of the powder pattern was only possible with the help of the theoretical powder pattern calculated from the crystal-structure data. Unit-cell parameters of skorpionite refined from the X-ray powder data for a monoclinic cell are a = 19.042(2), b = 9.309(1), c = 6.519(1) Å, β = 92.72(1)°, V = 1154.3(2) $Å^3$, which is in perfect agreement with the data obtained from the crystal structure determination. The powder diffraction pattern shows strong texture effects due to preferred orientation parallel to {100}. Observed intensities have been corrected for texture effects according to the March model (Deyu *et al*., 1990); these are given in Table 2 together with the original intensity data.

Single-crystal structure determination

For single-crystal X-ray investigation served a thin, tabular and lath-like crystal of skorpionite that was elongated parallel to [001] and flattened on (100). Details of the data collection and structure refinement are compiled in Table 3. The crystal system is monoclinic, the space group was found from the extinction rules and structure refinement to be $C2/c$. The atomic positions of the Zn, Ca and P atoms were located by direct methods (Sheldrick, 1997a). Successive Fourier and difference Fourier maps revealed the oxygen and carbon atoms (Sheldrick, 1997b). Atom labels O_p, O_c, O_h and O_w represent oxygen atoms of the phosphate, carbonate and hydroxyl group and the water molecule, respectively. The atoms Ca1, C, O_c1 and O_w are located at the two-fold axes, the atoms Ca2 and O_c2 as well as that belonging to the phosphate group are at general positions. For all these atoms structural parameters including anisotropic displacement parameters were refined. At this stage a high anisotropy for the O_w atom was observed with the maximum elongation approximately parallel to [001]. Successively it was removed from the special position at the two-fold axis, and then split into two general positions and refined successfully (the resulting occupation factor is 0.25). However, large anisotropies were maintained reflecting strong dislocation phenomena. Also the principal mean square atomic displacement of the O_c1 atom is worthy to note whereas those of the other atoms are quite reasonable. Trials to refine structure models with

Table 2. X-ray powder diffraction data[1] of skorpionite.

h	k	l	d_{calc}	I_{calc}	d_{obs}	I^2_{obs}	$I^2_{obs(corr.)}$
2	0	0	9.510	99	9.501	53	53
1	1	0	8.361	4	8.342	1	9
3	1	0	5.240	27	5.238	10	30
1	1	–1	5.190	6			
4	0	0	4.755	4	4.754	4	4
2	2	0	4.181	2	4.179	1	7
3	1	–1	4.163	2			
0	2	1	3.787	22	3.785	2	20
2	2	–1	3.552	4	3.551	1	9
2	2	1	3.485	7	3.486	1	10
4	2	0	3.326	2	3.323	2	9
0	0	2	3.256	2	3.256	1	5
6	0	0	3.170	100	3.170	100	100
5	1	–1	3.156	6			
2	0	–2	3.126	2			
1	3	0	3.063	22	3.063	6	42
1	1	–2	3.056	14			
2	0	2	3.037	16	3.037	2	19
1	1	2	3.013	63	3.014	5	54
4	2	–1	3.003	4			
3	3	0	2.787	46	2.788	14	67
1	3	1	2.763	7			
4	0	–2	2.748	4	2.747	1	7
3	1	2	2.718	11	2.719	2	12
0	2	2	2.668	3	2.666	1	3
4	0	2	2.629	4	2.628	1	5
2	2	–2	2.595	23	2.595	2	20
3	3	–1	2.582	24	2.582	3	21
6	2	–1	2.464	3	2.461	2	2
7	1	–1	2.460	3			
5	1	–2	2.445	8	2.446	1	7
5	3	0	2.405	9	2.405	4	16
7	1	1	2.384	3	2.382	1	2
4	2	–2	2.366	16	2.366	2	14
5	1	2	2.339	3	not obs.		
4	2	2	2.289	2	not obs.		
2	4	0	2.261	7	2.260	2	21
1	3	–2	2.239	4	not obs.		
0	4	1	2.191	19	2.192	2	21
1	1	–3	2.112	11	2.111	1	9
7	1	–2	2.083	6	2.082	1	4
9	1	0	2.061	5	2.061	3	4
7	3	0	2.044	5	2.044	2	8
8	2	–1	2.039	9	2.039	2	7
3	1	–3	2.034	2			
4	4	–1	2.003	4	1.992	4	15
9	1	–1	1.992	6			
7	1	2	1.992	26			
8	2	1	1.989	2			
3	1	3	1.978	4			
2	2	–3	1.943	4	1.931	1	6
7	3	1	1.931	5			
2	2	3	1.910	4	1.906	1	7
0	4	2	1.893	4			

Table 2. Cont.

h	k	l	d_{calc}	I_{calc}	d_{obs}	I^2_{obs}	$I^2_{obs(corr.)}$
8	0	2	1.878	4	1.877	1	5
6	4	0	1.876	2			
2	4	–2	1.867	4	not obs.		
2	4	2	1.847	9	1.847	1	11
6	4	–1	1.816	4	1.810	2	7
8	2	–2	1.810	14			
6	4	1	1.789	2	1.786	1	12
1	5	–1	1.784	7			
1	5	1	1.780	5			
1	3	–3	1.777	3			
4	4	–2	1.776	3			
1	3	3	1.765	5			
7	3	–2	1.760	3			
9	3	0	1.747	17	1.746	5	17
4	4	2	1.743	4			
8	2	2	1.742	2			

[1] Philips X'Pert powder diffractometer, Cu$K\alpha$ radiation; reflection mode; internal standard: Si. I_{calc} calculated with LAZY PULVERIX (Yvon *et al*., 1977); reflections with $I_{calc} \geq 2$ are listed.

[2] The powder diffraction pattern shows strong texture effects due to preferred orientation parallel to {100}. Observed intensities I_{obs} are not corrected for texture effects. Intensities $I_{obs(corr.)}$ are corrected according to the March model (Deyu *et al*., 1990); March coefficient 0.59.

split positions for the O_c1 atom did not improve the final results. Three H atoms were located experimentally. One H atom belongs to the hydroxyl group (H_h); the two others (H_w1 and H_w2) to the water molecule. The position H_w1 is fully occupied (site symmetry 2). H_w2 is at a general position but only half occupied; however, its atomic coordinates and the isotropic displacement parameter could be refined without problems. The structural parameters and the bond valence parameters according to Brese & O'Keeffe (1991) are given in Table 4. The electron density in the final difference Fourier map varies from –1.05 to +1.09 eÅ^{-3}; the highest peaks are in the surrounding of the Zn atoms and along the P–O bonds; the latter reflect the pronounced covalent bond character between P and O atoms.

Results and discussion

The crystal structure of skorpionite is characterized by a three-dimensional network of a couple of distinct structural units (Fig. 5). The size and shape of all coordination figures are in agreement with common crystal chemical experience (*cf.* Table 5). The atomic arrangement can be described topologically as an alternate stacking of neutrally charged $[Ca2_2Zn_2(OH)_2(PO_4)_2]^\circ$ and $[Ca1(CO_3)(H_2O)]^\circ$ layers parallel to (100). They are linked by the hydrogen bond formed by the hydroxyl group and by Ca–O bonds. This arrangement reflects the tabular morphology of the crystals.

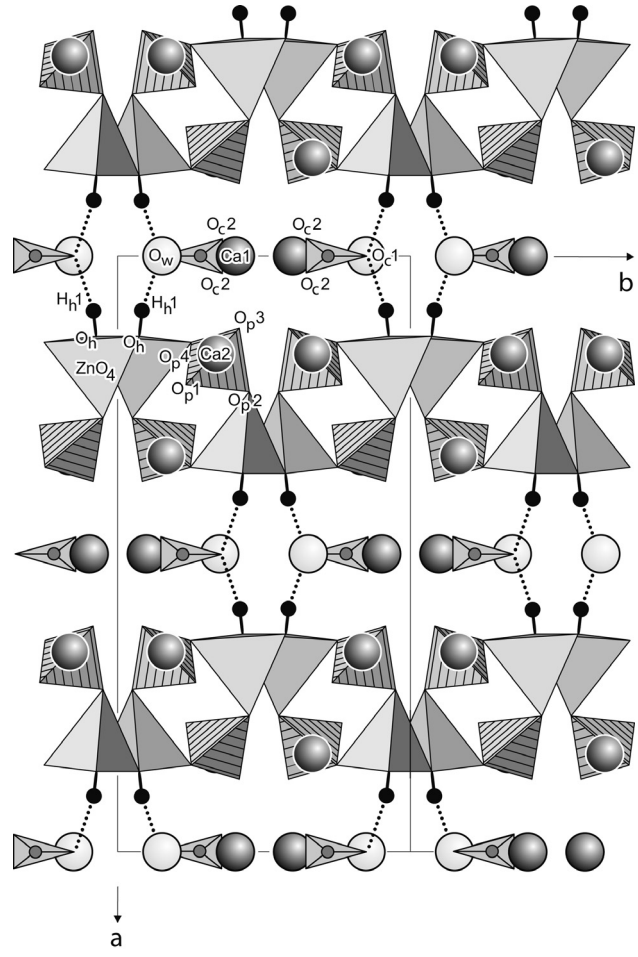

Fig. 5. The crystal structure of skorpionite in a projection parallel to [001]. The tetrahedra $[P(O_p)_4]^{3-}$ and $[Zn(O_p)_3(O_h)]^{6-}$ are hatched and shaded respectively. The $[C(O_c)_3]^{2-}$ groups are represented by triangles with the carbon atom in the centre. Dark grey balls represent the Ca1 and Ca2 atoms, light grey balls the average position of the O_w atoms. For clarity, only the hydrogen bonds O_h–H_h···O_c1 are indicated but O_w–H_w1/ H_w2···O_c1 are omitted.

The Ca1 atom has point symmetry 2, it is [7] coordinated in form of a remarkable regular pentagonal *bi*pyramid; the equatorial plane is approximately parallel to (100) and consists of one O_w and four O_c2 atoms (Fig. 6). The bond angles O_c2–Ca1–O_c2/O_w are 72(1) to 87(2)°; the large standard deviations result from the inaccuracy of the position of the O_w atoms. Two O_p3 atoms represent the apices of the coordination polyhedron; the bond angles between the O atoms within the equatorial plane and the apices vary between 77.83(4) and 103.36(4)°; that between the two apices amounts 173.60(6)°. Rows parallel to [001] are built by edge-sharing of the *bi*pyramids (O_c2–O_c2 = 3.218(2) Å). Within the equatorial ring one O_c2–O_c2 edge of 2.223(2) Å is in common with the carbonate group. The third corner of the carbonate group (atom O_c1) acts as the acceptor atom of all hydrogen bonds within the crystal structure of $Ca_3Zn_2(PO_4)_2(CO_3)(OH)_2 \cdot H_2O$. The carbonate group is planar within the accuracy of the structure refinement. The

Table 3. Single-crystal Xray data collection and structure refinements of skorpionite, $Ca_3Zn_2(PO_4)_2CO_3(OH)_2\square H_2O$.

a [Å]	19.045(3)
b [Å]	9.320(2)
c [Å]	6.525(1)
β [°]	92.73(2)
V [Å^3]	1156.9
Z	4
ρ_{calc} [g cm^3]/μ(Mo$K\alpha$) [mm^{-1}]	3.18/5.84
crystal dimensions [μm]	25 × 40 × 250
range of data collection ($\pm h \pm k \pm l$) [°]	$3 < 2\vartheta < 70$
number of images / rotation angle per image [°]	720/2
scan mode (at 14 distinct ω-angles)	ϕ-scans
scan time [s/°] / frame size (binned mode)	160/621×576 pixels
detector-to-sample distance [mm]	30
measured reflections	9831
unique reflections (n) / reflections with $F_o > 4\sigma(F_o)$	2550/2282
$R_{int} = \Sigma\lvert F_o^2 - F_o^2(\text{mean})\rvert/\Sigma F_o^2$	0.022
extinction parameter	0.0007(2)
$R1 = \Sigma(\lvert\lvert F_o\rvert - \lvert F_c\rvert\rvert)/\Sigma F_o$ (2551/2283 reflections)	0.022/0.027
$wR2 = [\Sigma w(F_o^2 - F_c^2)^2 / \Sigma\lvert wF_o^4]^{1/2}$	0.058
GooF = $\{\Sigma[w(F_o^2 - F_c^2)^2] / (n - p)\}^{0.5}$	1.049
max Δ/σ; number of variable parameters (p)	< 0.001; 126
final difference Fourier map [eÅ^{-3}]	–1.05 to +1.09

NONIUS four-circle diffractometer equipped with a CCD detector and a 300 μm capillary-optics collimator (Mo tube, graphite monochromator). Unit-cell parameters were obtained by least-squares refinements of 2ϑ values. Corrections for Lorentz, polarization and absorption effects (multi-scan method); complex scattering functions for H^{1-} and neutral Zn, Ca, P, C and O atoms (Wilson, 1992); programs Collect (Nonius, 1999; Otwinowski & Minor, 1997), SHELXS-97, SHELXL-97 (Sheldrick, 1997a,b).

$w = 1 / \{ \sigma^2(F_o^2) + [0.030\times P]^2 + 1.68\times P\}$; $P = ([\max(0,F_o^2)] + 2 \times F_c^2) / 3]$.

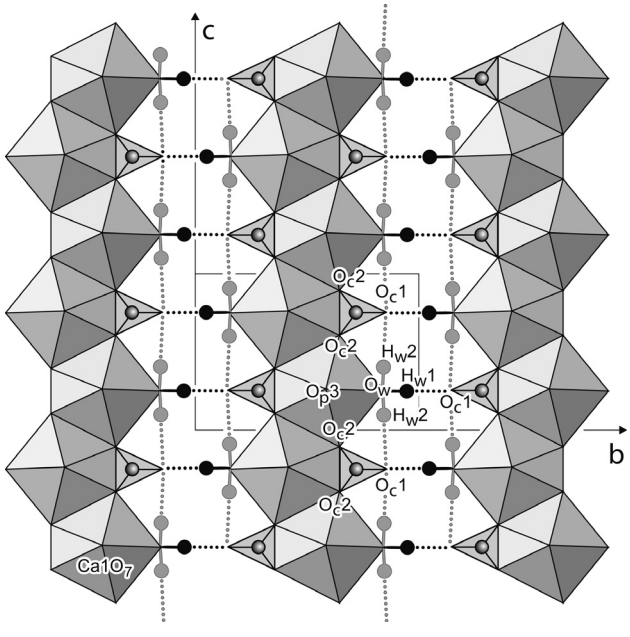

Fig. 6. Skorpionite: the $[Ca1(CO_3)(H_2O)]^\circ$ layers parallel to (100) with $-0.15 < x < 0.15$ in a projection parallel [100]. Only the average position of the O_w atom is indicated. The H_w2 position is only half occupied.

average C–O bond length of 1.290 Å agrees with the mean value of 1.284 Å recalculated from 34 carbonate groups in well refined crystal structures (Zemann, 1981).

The Zn and P atoms are both tetrahedrally coordinated to oxygen atoms. Besides the different size (the average bond distances ⟨ P–O ⟩ and ⟨ Zn–O ⟩ are 1.5380 and 1.9665 Å), the PO_4 tetrahedron is more regular as compared to the ZnO_4 tetrahedron; O–P–O varies from 105.43(6) to 112.01(7)° whereas O–Zn–O from 87.42(4) to 130.16(5)°. It is a common crystal chemical experience that the larger coordination polyhedra are less regular within a crystal structure. The distinct irregularities are reflected in the distortion parameters (Baur, 1974). The distortions of the bond distances ($DI_d = (\sum_{i=1}^{n1} |d_i - d_m|)/n_1 \cdot d_m$) and bond angles ($DI_\angle = (\sum_{i=1}^{n2} |\angle_i - \angle_m|)/n_2 \cdot \angle_m$) are 0.0051 / 0.0194 for PO_4 and 0.0198 / 0.0843 for ZnO_4 tetrahedra, respectively.

The ZnO_4 tetrahedra are corner connected to pyroxene-like $[Zn(O_p)_2O_h]^{4-}$ zweier-single chains running parallel to [001] (Fig. 7). The shared corner is the oxygen atom of the hydroxyl group; the Zn–O_h–Zn bond angle is 119.08(5)°. This value is significantly smaller as compared to silicates (Nyfeler *et al.*, 1995). The chains are linked by the phosphate tetrahedra to corrugated layers centred in x = 1/4 and 3/4. The Zn–O_p2/O_p4–P bond angles are 128.56(7) and 121.02(6)°. Topologically, the layers are formed from four- and eight-membered rings. The former are built from alternatingly arranged ZnO_4 and PO_4 tetrahedra. The latter consist of each three ZnO_4 tetrahedra in neighbouring $[Zn(O_p)_2O_h]^{4-}$ chains linked by opposite PO_4 tetrahedra. Networks formed by the corner-connection of tetrahedra are common for silicates; among them, four- and eight-membered rings are common (*e.g.* in feldspars). For Zn

Table 4. Fractional atomic coordinates and displacement parameters of skorpionite. The anisotropic displacement parameters are defined as: $\exp[-2\pi^2 \Sigma_{i=1}^{3} \Sigma_{j=1}^{3} U_{ij} a_i^* a_j^* h_i h_j]$, U_{equiv} according to Fischer & Tillmanns (1987). Sums of bond valences v according to Brese & O'Keeffee (1991); only the contribution between the oxygen atoms and the cations Zn, Ca, P and C are considered.

	site occupation	site symmetry	x	y	z	U_{equiv}/U_{iso}	U_{11}	U_{22}	U_{33}	U_{23}	U_{13}	U_{12}	v
Zn	1.0	1	0.170688(9)	0.04391(2)	0.41120(3)	0.01552(6)	0.01380(8)	0.01906(10)	0.01365(9)	0.00474(6)	0.00023(6)	–0.00242(6)	1.98
Ca1	1.0	2	0	0.59791(4)	¼	0.01225(7)	0.01049(14)	0.01400(16)	0.01221(16)	0	0.00018(11)	0	2.16
Ca2	1.0	1	0.164189(14)	0.33537(3)	0.12171(4)	0.01213(6)	0.01232(11)	0.01235(12)	0.01180(11)	0.00159(8)	0.00120(8)	0.00026(8)	1.95
P	1.0	1	0.178044(18)	0.66662(4)	0.15062(5)	0.01057(7)	0.01002(13)	0.01247(15)	0.00924(14)	0.00006(10)	0.00058(10)	–0.00065(10)	4.78
C	1.0	2	0	0.2818(2)	¼	0.0136(3)	0.0134(7)	0.0137(8)	0.0138(8)	0	0.0031(6)	0	3.93
O_p1	1.0	1	0.21612(5)	0.76680(13)	0.3030(2)	0.0160(2)	0.0148(4)	0.0212(5)	0.0118(4)	–0.0024(4)	–0.0005(3)	–0.0046(4)	1.78
O_p2	1.0	1	0.22778(6)	0.55013(12)	0.0690(2)	0.0154(2)	0.0125(4)	0.0145(4)	0.0195(5)	–0.0010(4)	0.0028(3)	0.0006(3)	2.02
O_p3	1.0	1	0.12142(5)	0.58406(12)	0.2629(2)	0.0148(2)	0.0111(4)	0.0188(5)	0.0146(4)	0.0023(4)	0.0020(3)	–0.0018(3)	1.94
O_p4	1.0	1	0.14517(6)	0.74825(12)	–0.0352(2)	0.0150(2)	0.0175(4)	0.0159(4)	0.0115(4)	0.0018(3)	–0.0019(3)	–0.0002(3)	1.90
O_c1	1.0	2	0	0.14635(18)	¼	0.0238(3)	0.0209(7)	0.0124(7)	0.0390(10)	0	0.0109(7)	0	1.41[c]
O_c2	1.0	1	0.02937(6)	0.35493(12)	0.1068(2)	0.0157(2)	0.0161(4)	0.0184(5)	0.0128(4)	0.0017(4)	0.0025(3)	–0.0023(4)	1.98
O_h	1.0	1	0.13476(5)	0.07351(12)	0.1247(2)	0.0131(2)	0.0122(4)	0.0152(4)	0.0119(4)	–0.0016(3)	0.0011(3)	0.0013(3)	1.26[a]
O_w1	0.25	1[d]	0.000(3)	0.850(2)	0.201(6)	0.033(7)	0.063(12)	0.008(5)	0.028(12)	–0.008(4)	–0.011(11)	0.005(4)	0.33[b]
O_w2	0.25	1[d]	0.0110(16)	0.848(3)	0.216(6)	0.030(6)	0.046(8)	0.027(7)	0.016(10)	0.001(5)	0.009(7)	0.001(4)	0.39[b]
H_h	1.0	1	0.0928(13)	0.082(3)	0.134(4)	0.002(6)							
H_w1	1.0	2	0	0.924(6)	¼	0.018(14)							
H_w2	0.5	1	0.002(3)	0.851(7)	0.066(10)	0.018(17)							

[a] Donor of one hydrogen bond; [b] donor of two hydrogen bonds; [c] acceptor of three hydrogen bonds; [d] average symmetry 2.

Table 5. Interatomic bond lengths (Å) and bond angles (°) of skorpionite.

Ca1–$O_p3^{0,iii}$	2.3136(11)	Zn–O_h^{ii}	1.9230(11)	P–O_p1	1.5224(11)			
Ca1–$O_w2^{0,iii}$	2.35(2)	Zn–O_p2^{vii}	1.9327(11)	P–O_p3	1.5386(11)			
Ca1–$O_w1^{0,iii}$	2.38(2)	Zn–O_h	1.9790(11)	P–O_p4	1.5392(11)			
Ca1–$O_c2^{iv,v}$	2.4088(11)	Zn–O_p4^{v}	2.0314(12)	P–O_p2	1.5516(11)			
Ca1–$O_c2^{0,iii}$	2.5226(13)	⟨ Zn–O ⟩	1.9665	⟨ P–O ⟩	1.5380			
⟨ $Ca1^{[10]}$–O ⟩	2.4025	O_h^{ii}–Zn–O_p2^{vii}	110.98(5)	O_p1–P–O_p2	111.95(6)			
		O_h^{ii}–Zn–O_h	130.14(5)	O_p1–P–O_p3	108.57(6)			
Ca2–O_p2	2.3729(12)	O_h^{ii}–Zn–O_p4^{v}	108.76(5)	O_p1–P–O_p4	112.00(7)			
Ca2–O_p1^{vii}	2.3957(11)	O_p2^{vii}–Zn–O_h^{ii}	111.02(5)	O_p2–P–O_p3	105.47(6)			
Ca2–O_p4^{v}	2.4138(11)	O_p2^{vii}–Zn–O_p4^{v}	101.93(4)	O_p2–P–O_p4	107.91(6)			
Ca2–O_h	2.5044(12)	O_h –Zn–O_p4^{v}	87.41(4)	O_p3–P–O_p4	110.76(6)			
Ca2–O_p1^{vi}	2.5308(12)							
Ca2–O_p3^{vi}	2.5546(12)	C–O_c1	1.262(3)	O_w1···O_w1^{iii}	0.63(8)			
Ca2–O_c2	2.5714(12)	C–$O_c2^{0,iii}$	1.304(2)	O_w2···O_w2	0.62(6)			
Ca2–O_p3	2.6375(12)	⟨ C–O ⟩	1.290	O_w1···O_w2^{iii}	0.588(14)			
⟨ $Ca2^{[8]}$–O ⟩	2.4976	O_c1–C–$O_c2^{0,iii}$	121.53(9)					
		O_c20–C–O_c2^{iii}	116.94(18)					
Hydrogen bonds								
Donor	H atom	Acceptor	D–H	H···A	D···A	D–H···A	water molecule	
O_h	H_h	O_c1	0.81(3)	2.04(3)	2.8134(12)	159(3)		
O_w1	H_w1	O_c1^{i}	0.76(6)	2.07(5)	2.78(2)	156(3)	H_w1–O_w1–H_w2	114(5)
O_w1	H_w2	O_c1^{iv}	0.89(8)	2.06(7)	2.81(3)	176(3)	O_c1^{i}···O_w1···O_c1^{iv}	96(1)
O_w2	H_w1	O_c1^{i}	0.77(5)	2.07(5)	2.79(2)	155(3)	H_w1–O_w2–H_w2	103(6)
O_w2	H_w2	O_c1^{iv}	1.00(7)	2.06(7)	2.91(3)	176(3)	O_c1^{i}···O_w2···O_c1^{iv}	93(1)

Symmetry code: not specified and ^{0} x, y, z; ^{i} $x, y+1, z$; ^{ii} $x, -y, -z+1/2$; ^{iii} $-x, y, -z+1/2$; ^{iv} $-x, -y+1, -z$; ^{v} $x, -y+1, z+1/2$; ^{vi} $x, -y+1, z-1/2$; ^{vii} $-x+1/2, y-1/2, -z+1/2$

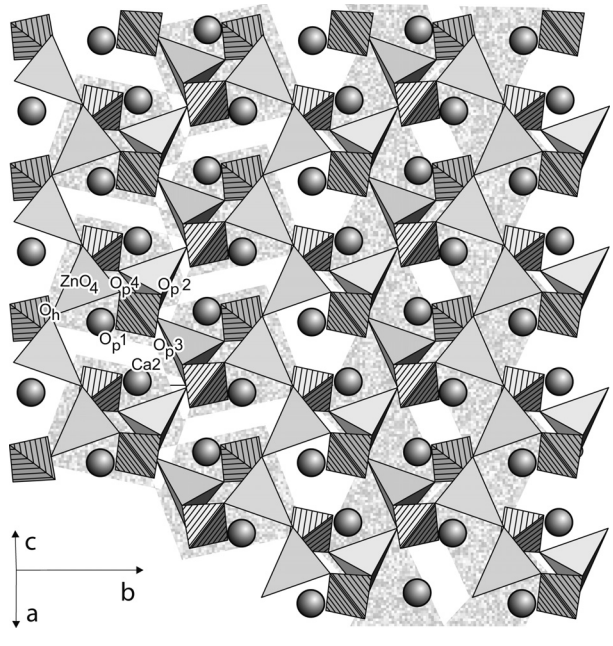

Fig. 7. Skorpionite: the slab $[Ca2_2Zn_2(O_h)_2(PO_4)_2]^{\circ}$ parallel to (100) with $0.10 < x < 0.40$ in a projection parallel to ~ [101]. The four-membered rings within these layers $[Zn_2(O_h)_4(PO_4)_2]^{\circ}$ (left side) and the pyroxene-like chain $[Zn(O_h)(O_p)_2]^{4-}$ (right side) are indicated. The tetrahedra $[P(O_p)_4]^{3-}$ and $[Zn(O_p)_3(O_h)]^{6-}$ are hatched and shaded respectively. Dark grey balls represent the Ca1 atoms. For clarity, H_h atoms are omitted; O_h atoms link the $[Zn(O_p)_3(O_h)]^{6-}$ tetrahedra.

atoms a variety of coordination numbers ranging from [4] to [6] are known. Zinc arsenates with a tetrahedral network based on a combination of four- and eight-membered rings occur in zeolite-like compounds like $(NH_4)ZnAsO_4$ (Feng, 2001) and $Cs_3Zn_4O(AsO_4)_3{\cdot}4H_2O$ (Harrison *et al.*, 2000), but also in $LiZnAsO_4{\cdot}H_2O$ (Jensen *et al.*, 1998) or $Sr(ZnAsO_4)_2$ (Lucas, 1998).

Two Ca2 atoms are located at the top and bottom faces of the larger 8-membered rings. They are [8] coordinated and form pairs of edge-shared (O_p1–O_p1) tetragonal antiprisms with O_p1–O_p3–O_p2–O_h and O_p1–O_p2–O_p3–O_p4 as the top and bottom faces (Fig. 8). The average ⟨ Ca2–O ⟩ bond length of 2.4976 Å is somewhat larger as compared to ⟨ Ca1–O ⟩ which amounts 2.4025 Å; the difference is expected from the distinct coordination numbers [7] and [8], respectively (Blatov *et al.*, 1999). The $Ca2_2O_{14}$ dimers are corner-linked (atoms O_p3) among each other. Two of the O–Ca2–O bond angles enclosing edges of the $Ca2O_8$ polyhedron amount independently 58.51(4)°; they are decreased because the edges are shared with the phosphate tetrahedron (O_p2–O_p3; O_p1–O_p3); the other O–Ca2–O bond angles are 70.75(4) to 84.67(4)° within the square top and bottom faces of the CaO_8 polyhedron and 68.06(4) to 88.64(4)° between them.

The approximate position of the oxygen atom of the water molecule (O_w) is the special position (0 0.85 1/4) located at the twofold axis. During the first stage of structure refinement large anisotropies of the dislocation parameter indicated splitting along [001]. Refinements were tried for

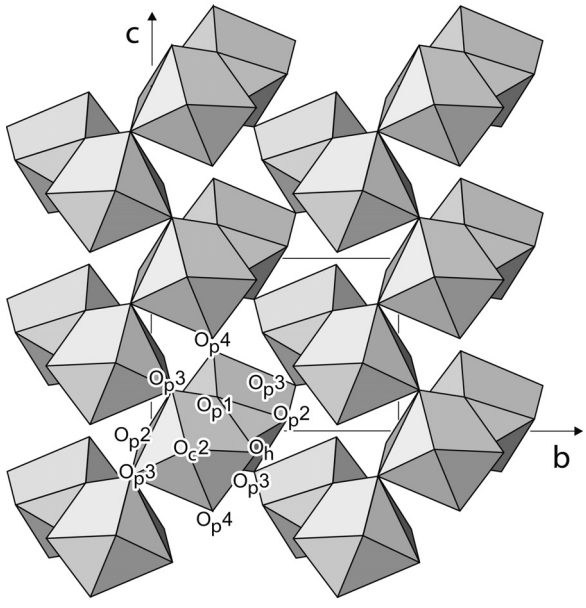

Fig. 8. Skorpionite: the connection of the square antiprisms $[Ca2(O_h)(O_c)(O_p)_6]^{-14}$ to layers parallel to (100) in a projection parallel to [100].

different models with the O_w atom displaced from the special position and with split positions as well. The displacement of the O_w atom from the ideal position is caused by the lengths of the hydrogen bonds and by the geometry of the water molecule: the average hydrogen bond O_w–$H_w1\cdots O_c1$ is located along the two-fold axis. O_w–$H_w1\cdots O_c1$ of 2.76 Å is a moderate hydrogen-bond length. Considering the average position of the O_w atom, O_w–$H_w2\cdots O_c1$ is much longer (3.26 Å) and $O_c1\cdots O_w\cdots O_c1$ is about 90° which differs largely from the 105° expected within the water molecule. Shifting of the O_w atom adopts both, a shorter O_w–$H_w2\cdots O_c1$ bond length and a larger $O_c1\cdots O_w\cdots O_c1$ bond angle. However, the position of the O_w atom is very inaccurate due to the high dislocation which is larger as compared to that of the H_w atoms. The O_c1 atom is the only atom in the crystal structure which acts as an acceptor atom of the hydrogen bonds. As a response to the partial occupation of O_w1 and O_w2 position and the relative long hydrogen bond length, O_c1 shows a displacement mainly in the direction [001], *i.e.* in the direction towards to the O_w atom. Models with a split O_c1 site did not improve the results.

Acknowledgements: The authors thank D. Ewald for the powder diffraction measurements, G. Blass for EDX analyses, E. Jägers for the FTIR spectra, E. Libowitzky for the Raman spectra, and K. Kärner for the SEM micrograph. Samples for investigation were kindly provided by L. Krahn.

References

Baur, W.H. (1974): The geometry of polyhedral distortions. Predictive relationships for the phosphate group. *Acta Crystallogr.*, **B30**, 1195-1215.

Blatov, V.A., Pogildyakova, L.V., Serezhkin, V.N. (1999): Analysis of the environment of beryllium, magnesium and alkaline earth atoms in oxygen-containing compounds. *Acta Crystallogr.*, **B55**, 139-146.

Borg, G., Kärner, K., Buxton, M., Armstrong, R., Merwe, S. van der (2003): Geology of the Skorpion supergene zinc deposit, Southern Namibia. *Econ. Geol.*, **98**, 749-771.

Braithwaite, R.S.W., Mereiter, K., Paar, W.H., Clark, A.M. (2004): Herbertsmithite, $Cu_3Zn(OH)_6Cl_2$, a new species, and the definition of paratacamite. *Mineral. Mag.*, **68**, 527-539.

Braithwaite, R.S.W., Pritchard, R.G., K., Paar, W.H., Pattrick, R.A.D. (2005): A new mineral, zincolibethenite, $CuZnPO_4OH$, a stoichiometric species of specific site occupancy. *Mineral. Mag.*, **69**, 145-153.

Brese, N.E. & O'Keeffe, M. (1991): Bond-valence parameters for solids. *Acta Crystallogr.*, **B47**, 192-197.

Deyu, L., O'Connor, B.H., Roach, G.I.D., Cornell, J.B. (1990): Use of X-ray powder diffraction Rietveld pattern-fitting for characteristic preferred orientation in gibbsite. *Powder Diffr.*, **5**, 79-85.

Feng, P.-Y., Zhang, T.-Z., Bu, X.-H. (2001): Arsenate zeolite analogues with 11 topological types. *J. Am. Chem. Soc.*, **123**, 8608-8609.

Fischer, R.X. & Tillmanns, E. (1987): The equivalent isotropic displacement factor. *Acta Crystallogr.*, **C44**, 775-776.

Harrison, W.T.A., Phillips, M.L.F., Bu, X.-H. (2000): Synthesis and single-crystal structure of $Cs_3Zn_4O(AsO_4)_3{\cdot}4H_2O$, an open-framework zinc arsenate. *Micropor. Mesopor. Mat.*, **39**, 359-365.

Hovestreydt, E. (1983): On the atomic scattering factor for O^{2-}. *Acta Crystallogr.*, **A39**, 268-269.

Jacob, J., Ward, J.D., Bluck, B.J., Scholz, R.A., Frimmel. H.E. (2006): Some observations on diamondiferous bedrock gully trapsites on Late Cainozoic, marine-cut platforms of the Sperrgebiet, Namibia. *Ore Geol. Rev.*, **28**, 493-506.

Jensen, T.R., Norby, P., Norlund Christensen, A., Hanson, J.C. (1998): Hydrothermal synthesis, crystal structure refinement and thermal transformation of $LiZnAsO_4{\cdot}H_2O$. *Micropor. Mesopor. Mat.*, **26**, 77-87.

Kärner, K. (2006): The metallogenesis of the Skorpion non-sulphide zinc deposit, Namibia. Dissertation, Martin Luther University, Halle-Wittenberg, Germany, 252 p. (in English).

Kärner, K., Borg, G., Harney, D., Hartmann, K. (2002): A description of first ore minerals from the open pit at the non-sulphide Skorpion Mine, Namibia. 11th Symposium of IAGOD & GEOCONGRESS 2002, Windhoek, July 2002.

Lucas, F., Elfakir, A., Wallez, G., Quarton, M., Lagache, M. (1998): Synthesis and Rietveld refinement of new phosphate and arsenate analogues of paracelsian. *Can. Mineral.*, **36**, 1045-1051.

Mandarino, J.A. (1981): The Gladstone-Dale relationship: part IV. The compatibility concept and its application. *Can.Mineral.*, **19**, 441-450.

Nonius, B.V. (1999): "Collect". Data collection software. Brucker AXS, http://www.brucker-axs.de/.

Nyfeler, D., Armbruster, T., Dixon, R., Bermanec, V. (1995): Nchwaningite, $Mn_2^{2+}SiO_3(OH){\cdot}H_2O$, a new pyroxene-related

chain silicate from the N'chwaning mine, Kalahari manganese field, South Africa. *Am. Mineral.*, **80**, 377-386.

Otwinowski, Z. & Minor, W. (1997): Processing of X-ray diffraction data collected in oscillation mode. In: C.W.J. Carter and R.M. Sweet, eds. *Method. Enzymol.*, **276**, 307-326.

Sheldrick, G.M. (1997a): SHELXS-97, a program for the solution of crystal structures. University of Göttingen, Germany.

— (1997b): SHELXL-97, a program for crystal structure refinement. University of Göttingen, Germany.

Sole, K.C., Feather, A.M., Cole, P.M. (2005): Solvent extraction in southern Africa: An update of some recent hydrometallurgical developments. *Hydrometallurgy*, **78**, 52-78.

Yvon, K., Jeitschko, W., Parthé, E. (1977): LAZY PULVERIX, a computer program, for calculating X-ray and neuron powder patterns. *J. Appl. Crystallogr.*, **10**, 73-74.

Wilson, A.J.C. (ed.) (1992): International Tables for Crystallography, Vol. C. Kluver, Dordrecht, The Netherlands.

Zemann, J. (1981): Zur Stereochemie der Karbonate. *Fortschritte Mineralogie*, **59**, 95-116.

Received 14 May 2007
Modified version received 15 August 2007
Accepted 29 November 2007